Synthetic birnessites and buserites as heavy metal cation traps and environmental remedies

Kledi Xhaxhiu [1],*

[1] Department of Chemistry, Faculty of Natural Sciences, Blv. "Zog I" No.2/1, 1001, Tirana Albania; E-Mail: kledi.xhaxhiu@unitir.edu.al

* Author to whom correspondence should be addressed; E-Mail: kledi.xhaxhiu@unitir.edu.al; Tel.: +35542229590 (ext. 123); Fax: +35542231120.
Received:7.8.2015 / Accepted:1.9.2015 / Published:1.10.2015

Microporous Na-birnessite-type manganese oxides are synthesized by oxidation of $Mn(OH)_2$ with $K_2S_2O_8$ in strong alkaline environment. Subsequent ion-exchange reactions in aqueous solutions containing Sr, Ba promote their incorporation into the layered structural frameworks, which upon further hydration lead to the respective layered Buserites. Chemical composition and surface structure are assessed by X-ray powder diffraction, nitrogen- and argon- sorptiometry. Na-birnessites and Sr-buserites display good crystallinity. Ba-buserites consist mainly of nanocrystals. Their N_2 adsorption/desorption isotherms of resemble IV-type isotherms. Integral and differential pore distribution curves obtained by N_2-sorptiometry exhibit out-of-layers pores of 4-5 nm and 10-20 nm. Na-birnessites, Sr- and Ba-buserites possess external B.E.T surfaces of 75.6, 49.2 and 93.6 m^2/g respectively. Considerable adsorption volumes of 14, 17 cm^3/g for P/P0 = 0.05 for Na-birnessites and Ba-buserites are assessed by Ar-sorptiometry. Differential pore distribution curves confirm inner-layer micropores of 5 to 7 Å with a B.E.T specific area of 76.2 m^2/g for Na-birnessites and 51.8 m^2/g for Ba-buserites. Na-birnessites and Sr-, Ba-buserites possess enhanced ionic exchanging capacity, acting as a "sink" for heavy metal cations such as Fe^{2+}, Fe^{3+}, Co^{2+}, Ni^{2+}, As^{3+}. The retention of U, Cs and Sr radioisotopes by them unfolds their salient anti-pollution potential for soil and subwater ecosystems.

Keywords: Na-birnessites, Sr-, Ba-buserites, one- and two-dimensional layers, porous media, adsorption/desorption properties, ion exchange capacity, heavy metal cation trap

1. Introduction

The history of the name birnessite derives from the region called Birness, from where Jones and Milne reported at first on this material [1]. It importance is related to the its manganese content which classify it as the main Mn-containing phase in soil, marine and nodules [1, 2]. Beyond this fact, what makes this mineral important is its characteristic two dimensional layered structure built of edge- and corner-sharing MnO_6 octahedral sheets separated by a single water molecule layer and random cations [4,5]. The latter cause a spacing varying from 7-7.1 Å [5]. Upon further hydrating at certain conditions they convert reversibly to buserites which have a similar structure but consist of two single molecule water layers enlarging the interlayer space around 10 Å [4,6,7]. Since water is loosely bound to the buserite structure, it can be lost easily upon drying yielding back birnessites [4,6,7]. This inter-conversion is of great importance for various topics and especially for manganese distribution in the nature. The special structure of birnessite and buserite bears several unusual properties such as pronounced adsorptive properties and ion exchanging [8-13]. In spite of the industrial applications of the latter [14-16, 17-20] deriving from this property, increasing interest is paid for their application as anticontamintats

[10,12,21,22] in the environmental remediation. Numerous studies have unveiled their adsorbing/exchanging capacities of various alkaline metal cations [7,10,8,24], transition metals cations [9,11,13,22,23] or even hazardous nuclear wastes containing uranium cations [5]. Due to the importance of these materials and their continuously reevaluation, this study aims to shed light on the structural and adsorptive properties of Na-birnessite and emphasise their cation sorptive/exchanging properties.

2. Results and Discussion

2.1 Structure of birnessites and buserites

Golden et al. were the first to report on the layered structure of birnessites. They found the chemical formula $Na_4Mn_{14}O_{27}*9H_2O$ for the synthetic Na-birnessites classifying it to the orthorhombic crystal system. The structure of Na-birnessite consisted of two-dimensional sheets of edge-shared MnO_6 octahedra, spaced at 7 Å and occupied by Mn^{3+}/Mn^{4+} species. This distance between layers could accommodate a single layer water molecules and exchangeable Na ions [6]. Latter studies of Le Goff et al. on Na-birnessites and buserites based on infrared and absorption spectroscopy investigations reported the chemical formula $Na0._{32}MnO_2*0.67H_2O$ for the dried Na-birnessite. Although the oxidation state of manganese is represented as 4, according to them it was merely 3.68 [4]. They could classify the Na-birnessite lamellar structure in the monoclinic space group of C2/m with Na ions and water molecules occupying the prismatic holes formed between the octahedral layers with a typical interlayer distance of 7.1. This interlayer distance reported by them was in full accordance to the previous investigations of Post and Veblen which determined the crystal structure of synthetic sodium, magnesium and potassium, birnessite using TEM and the Rietveld method [25]. Upon drying, Na-birnesites lose their single water molecule layer which leads to a decrease of the interlayer spacing of 5.6 Å [7]. Buserites in comparison to birnessites have a greater interlayer spacing of 9.3-10 Å [7], and contain double-water molecule layers between the two-dimensional edge-shared MnO_6 octahedral layers. They easily lose one water layer transforming to the respective stable Na-birnessites [4,7]. This transformation is interlaced with an interlayer shifting of approx. 0.3 Å. Due to the ability to maintain or lose the second water layer they are classified to unstable and stable buserites [7]. Buserites which lose reversibly one layer of water molecules upon drying and regain it upon stirring in water represent the unstable ones. Luo et al. showed that this process is strongly dependent on the preparation method and proposed a double aging method for the synthesis of stable Na-buserites at ambient conditions for longer times [7]. A schematic which summarizes all is described above on the reversible transformation dry-birnessite--birnessite-buserite is exhibited in fig. 1.

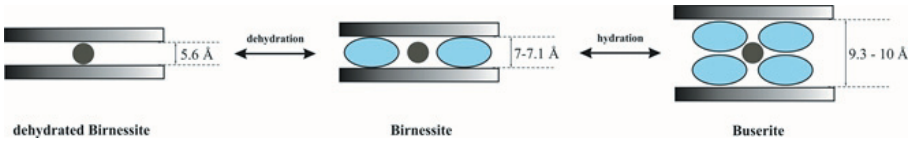

Figure 1: The reversible conversion of birnessite to dehydrated birnessite (left) and buserite (right). The top and bottom layers represent edge-sharing MnO_6 octahedra. The given distances between octahedral layers are based on the literatures [4,5,7].

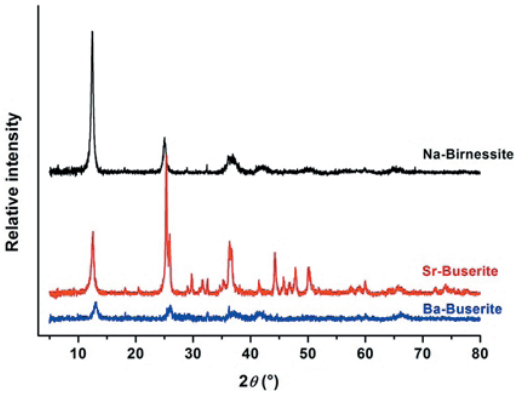

Figure 2: Measured XRD powder patterns of Na-birnessites, Sr- and Ba- busserites.

The measured diffraction pattern of Na-birnessites (Fig. 2) shows a good match with the pattern published by Prieto & Rives [26], which indexed and refined it in the monoclinic system with the lattice constants $a_0 = 5.039$ Å, $b_0 = 2.822$ Å, $c_0 = 7.366$ Å, $\beta = 103$ º. Indeed, literature data unveils that in most cases Na-birnessites crystallize in the monoclinic crystal system [4,27,28]. As reported by them, this is due to the high polarizing effect of the alkali cations (Li^+, Na^+, K^+) toward the water molecules which constrain the layered structure to maintain the monoclinic symmetry. The measured sample of Sr-buserite revealed a good crystallinity as shown by the powder pattern of fig. 2. In opposite to it, the powder pattern of Ba-buserite resembled more to XRD pattern of a nano-crystalline sample. Both diffraction patterns of measured buserites (Fig. 2) matched well to the measured pattern of Na-birnessites, especially for the position of the main reflections. This similarity to the diffraction pattern of Na-birnessites is due to the instability of Sr- and Ba-buserites at ambient conditions for long times as reported by Luo [7]. He found that Ba-buserite change direcly to Ba--birnessite upon drying, meanwhile Sr-buserite can retain the buserite structure up to 1 h after drying. For the latter, this conversion occurs gradually and partially. This fact explains the presence of some buserite structure reflections with low relative intensities, in the measured powder pattern of Sr-buserites.

2.2 Porosity and BET surface area

N_2 sorptiometric measurements were taken to determine the porosity and BET surface area of Na-birnessite, Sr- and Ba-buserite. The adsorption isotherms and the respective differential pore distributions are plotted in fig. 3. At the first glance, the adsorption isotherms of Na-birnessite (Fig 3a) and Ba-buserite (Fig. 3e) are characterized by a similar initial and maximal N_2 adsorption volume. Anyway, a close observation of the adsorption data unveils a light advantage of the initial and final adsorption volumes of Ba-buserite (13.32 cm^3/g vs. 15.91 cm^3/g) and (135.27 cm^3/g vs. 157.71 cm^3/g) making a difference in the adsorption volumes of approx. 20 cm^3/g.

Sr-buserites showed a poorer adsorption behavior in comparison to Na-birnessites and Ba-buserites. Its initial and final adsorption volumes consisted merely of 8.73 cm^3/g and 94.67 cm^3/g. The differential pore distributions of the measured samples (Fig. 3b,d,f) displayed the presence of the microporosity in all of them and an overall external porosity increasing in the order Sr-buserite < Na-birnessite < Ba-buserite. Since the N_2 kinetic molecule diameter is 3.64 Å [29] the N_2 molecule stericity impedes its entrance and accommodation in the free space between the interlayers, which in the case of Na-buserite in dried form is reported 1.94 Å. The BET specific surface area for these three samples was measured by this adsorbate and is shown in fig. 4. As expected and in full accordance to the adsorption isotherms and differential pore distributions, Ba-buserite shows the highest specific area 93.64 m^2/g followed by Na-birnessite with 75.57 m^2/g and Sr-buserite 49.16 m^2/g. Indeed, the determined BET specific surface area of Na-birnessites was slightly above the maximal border value of 72 m^2/g reported by Wong and Cheng [21] and much higher than the literature values [26,30]. To overcome the difficulty of the proper determination of the sample porosity due to the inaccessibility of N_2 entering the inlayer space of these materials, complementary

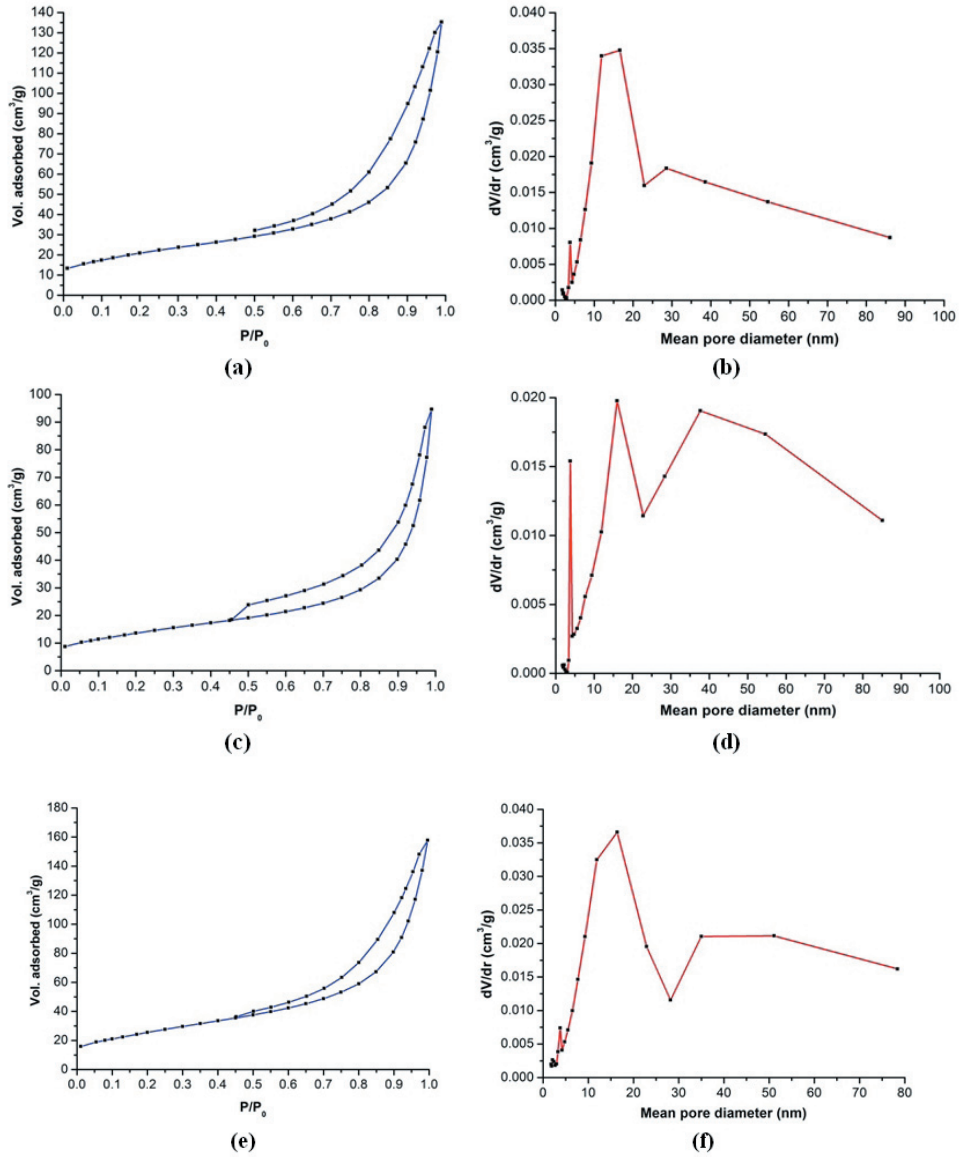

Figure 3: Adsorption desorption hysteresis of: (a) Na-birnessite, (c) Sr-buserite and (e) Ba-buserite; differential pore distribution of: (b) Na-birnessite, (d) Sr-buserite and (f) Ba-buserite.

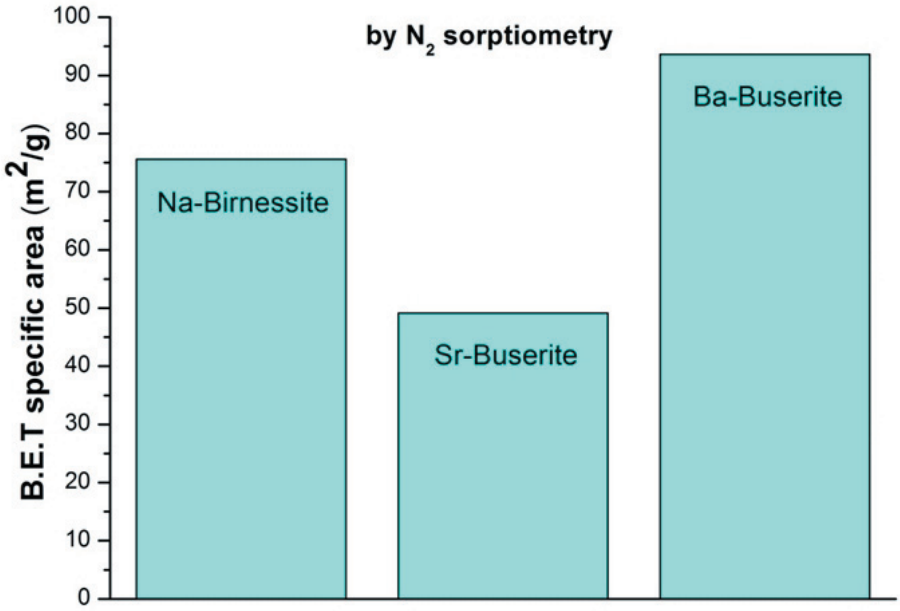

Figure 4: BET surface area of Na-birnessites, Sr- and Ba-buserites determined by N_2 sorptiometry.

Ar-sorptiometric measurements were taken for the samples of Na-birnessite and Ba-buserite. Ar atoms have a smaller kinetic diameter 3.4 [21] and hence can better access the pores. The Ar-adsorption isotherms of both samples were recorded for a relative pressure of 0.05 (Fig. 5a). The recorded Ar-adsorption isotherms exhibit slightly lower initial adsorption volumes compared to the N_2 adsorption data. Again Ba-buserite shows the highest adsorption volume of 17 cm^3/g, compared to 14 cm^3/g for Na-birnessite.

The differential pore distribution calculated according to the Horvath-Kawazoe equation (Fig. 5b) for both samples reveals the main pore distribution with mean diameters varying from 0.3 to 1.2 nm, and the maximum value at 7 Å. This is the most reported value of the interlayer distance in birnessites. This fact reinforces the conclusion regarding the instability of the Sr- and Ba-buserites at ambient conditions and emphasizes their partial or total conversion into the respective birnessites. These measurements also endorse the fact that the exchange of Na^+ with Ba^{2+} increases the porosity in the birnessite structure.

Complementary BET specific area determination based on Ar-sorptiometric measurements of Na-birnessite and Ba-buserite samples (Fig. 6) exhibited a larger BET specific area of the latter (60 vs. 64 m^2/g). Anyway these values are lower in comparison to the BET values reported above for the N_2-sorptric data and slightly above the value 55 m^2/g reported for Na-birnessite by Wong and Cheng [21]. The discrepancy between the BET surface area determined by N_2-sorptiometry and Ar-sorptiometry occurs due to the difference between the shapes of N_2 molecule and Ar atom, their polarisabilities and their surface packing behavior. Na-birnessite showed reveals a larger BET specific surface area compared to its external surface (60 m^2/g vs 57 m^2/g). The opposite was observed for Ba-buserites which showed a larger external surface area instead (64 m^2/g vs. 69 m^2/g).

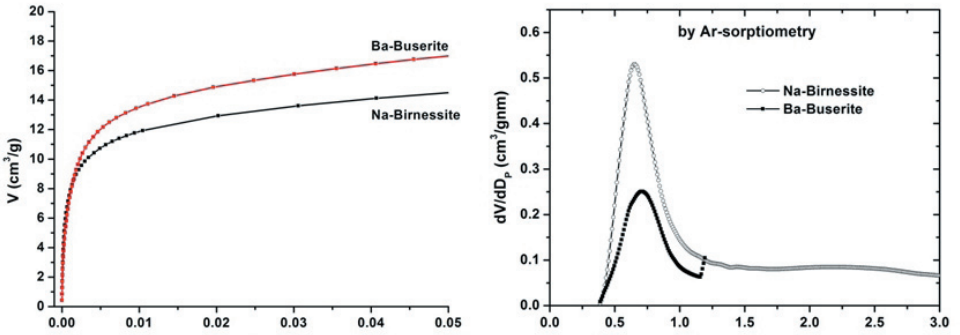

Figure 5: (a) Ar-adsorption isotherms of Na-birnessite and Ba-Buserite, (b) differential pore distribution of the samples of Na-birnessite and Ba-Buserite determined by Ar-sorptiometry.

The BET surface area determined for Ba-buserites is inferior in comparison to the approximate value 200 m^2/g reported by Jeffries and Stumm [8]. This indicates that the product obtained and reported in this study, claimed as Ba-buserite was probably an intermediate of Na-birnessite and Ba-buserite. This conclusion is fully endorsed by the finding of Luo et al. who reported the same while exchanging of Na with Ba in instable Na-buserite [7].

2.3 Cation exchanging and environmental protection

2.3.1 The role of birnessites

The physical properties of the nonstoichiometric manganese oxides, i.e. birnessites and buserites have a considerable effect on their adsorption properties. Although we didn't performed yet cationic adsorption studies with the synthesized materials, there is plenty of information in the literature reporting on the cationic adsorption/exchanging properties of birnessites and buserites. At one hand the cation adsorption in such layered materials occurs in the space between the octahedral layers. At the other hand, the cation exchanging process in them with the environmental cations occurs in two levels, namely a) exchanging with the cations situated between the octahedral layers, which is the quite frequent for most of them, b) exchanging with the manganese cations, occupying octahedral holes. The cation exchanging in birnessites and buserites has a considerable contribution in the environmental remedy. Rives, Arco and Prieto [10] reported on a partial cation exchange of Na- and K- containing birnessites when they were introduced to solutions containing Li^+, Mg^{2+} and Cu^{2+}. The reported exchanging order was $L^+ > Mg^{2+} > Cu^{2+}$. Since the cation exchange occurred between the interlayers ones and those introduced by the environment, it wasn't associated with the change of the interlayers spacing in them. Feng et al [11] found L-type adsorption isotherms of heavy metals from the aqueous environment. The adsorption was concentration dependent and increased sharply when the equilibrium concentration of the heavy metals was increased. From all the tested manganese oxides type structures, they reported on the enhanced adsorbing properties of birnessites toward Pb^{2+}, Cu^{2+} Zn^{2+}, Co^{2+} and Cd^{2+}. Lead was adsorbed the most followed by the others according to the given sequence. They also proposed that the cation adsorption process occurred in their hydroxylation form where the adsorbed amount was proportional to the respective hydrolysis constants. Table 1 exhibits the reported maximal adsorbed values for the mentioned cations.

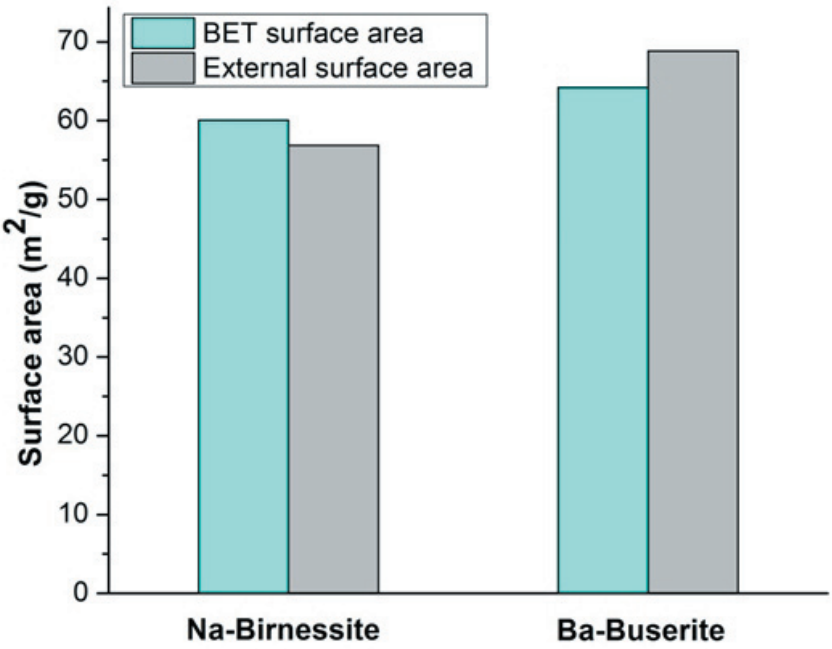

Figure 6: BET and external surface area of Na-birnessites, Sr- and Ba-buserites determined by Ar sorptiometry.

Adsorbing material	Maximal adsorption values of some heavy metals (mmol/kg)				
	Pb (0.396 nm)*	Co (0.35 nm)*	Cu (0.349 nm)*	Cd (0.371 nm)*	Zn (0.35 nm)*
Birnessite	148	189	190	168	189

Table 1: Maximal adsorption values of five heavy metals by birnessite [11].

The radius of the hydrated ion was calculated $r_{ion} + 2r_{H2O}$, rion was reported by Shannon [31]

Similar studies performed by McKenzie and Tebo et al. [9,23] in this field, revealed increased adsorption/exchanging capacities of birnesites toward the cationic species as follows $Pb^{2+} > Cu^{2+} > Co^{2+} > Ni^{2+} > Zn^{2+} > Mn^{2+} > Ca^{2+} > Mg^{2+}$. Manganese oxidation state plays the most important role in this sequence followed by the distributions of the cations in the layers and interlayers respectively [13,22]. Meanwhile, Villalobos et al. [32] found that the adsorption/exchanging capacity for Pb^{2+} among others was dependent on the birnessite specific area. According to Wong et al. [21] the great sorption capacity of Pb^{2+} in comparison to the other heavy metals is interlaced with its ability to occupy interlayer space in birnessite and their surface edge sites. All the adsorption/exchanging processes involving greater ions than the present ones are associated by the enlargement of the interlayer distance and birnessite cell distortion. Al-Attar and Dyer [5] reported increases of b-dimension in birnessite cell due to high uranium sorption

on Li-, Cs- and Ba-birnessites. Since the process is pH dependent, the best distribution coefficients values reported for Li- and Ca-birnessites in deionised water 2.71 x 106 and 1.67 x 106 ml/g respectively were achieve at pH = 6. In contrast to them, transition metal birnessites showed low adsorption/exchange values ranging between 34–184 ml/g.

Despite of the above distinctive exchanging properties between interlayer situated cations and the environmental ones, as mentioned previously, birnessites take part also to the cation exchanging between $Mn^{3+}/^{4+}$ occupying the octahedral holes and the environmental ones. In such process Mn plays the role of the oxidation agent. Feng et al. reported on the considerable amounts of Cr^{3+} adsorbed on birnessite reaching up to (1330.0 mmol/kg). The adsorption of Cr^{3+} occurring of at the interface induced new equilibria between it and Mn, leading to its further oxidation to Cr^{6+}. Due to the surface characteristics, once Cr^{6+} was formed it desorbed back from the birnessite surface into the solution. This process attributes to birnesites environmental remediation properties since Cr^{6+} is less toxic than Cr^{3+} [11]. Dias et al. [12] proved a similar behavior of synthetic birnessites toward As^{3+}. The contact of As^{3+} with the birnessite surface caused its direct oxidation to As^{5+} and the consequent reduction of Mn^{4+} to Mn^{3+} and Mn^{2+}. The maximal As^{3+} adsorption level reported by them was approx. 20 mg As/g.

2.3.2 The role of buserites

Similar to birnessites, busserites as their derivatives or precursors possess ion adsorption/exchange properties. Murray et al. [24] were the first to report on the adsorption/exchange of Ni^{2+}, Cu^{2+}, Co^{2+} Ca^{2+} at high concentrations from buserites. Jeffries and Stumm [8] reported later on the adsorption of two valent ions of Ca^{2+}, Zn^{2+} and Cu^{2+} from their aqueous solutions. At a pH values varying from 2-7 they found the following buserite adsorption sequence: $Ca^{2+} < Zn^{2+} < Cu^{2+}$. At normal pH values ranging from 6-8 buserites show enhanced adsorption capacities, decreasing considerably their concentrations in see waters. They also stressed the fact of the complicity of the heavy metal adsorption process regarding the released hydrogen ions from the surface. Later studies of Luo et al. [7] unveil the feasibility of obtaining stable buserites of Mg^{2+}, Ca^{2+}, and Sr^{2+} from Na-buserite. They demonstrated also the formation of stable buserites from the treatment of unstable Na-buserite with some transition metal cations, such as Mg^{2+}, Cu^{2+}, Zn^{2+}, Ni^{2+}, Co^{2+}, and Mn^{2+}.All these latter buserites formed, although considered stable at ambient conditions, upon heating they displayed higher instability in comparison to Mg-busserites. The latter were obtained very quick due to ion exchange from the unstable buserite. Different from all of these, the exchange of Na with Ba led to the formation of an intermediate product between birnessite and busserite. All of this cationic adsorption exchanges similar to birnessites were related with significantly increased interlayer spacing.

3. Experimental Section

We reported in this study the synthesis of Na--birnessite and the attempt of the synthesis of Sr- and Ba-buserites. The synthesized samples revealed significant differences in their XRD powder patterns. The XRD pattern of the Na--birnessites matched well with the literature reported pattern, assigning it hence to the monoclinic system. The claimed Sr- and Ba-buserite patterns displayed also close similarities with reported ones. The N_2 adsorption measurements unveiled the presence of micropores in all samples. The overall external porosity of them increased in the order Sr-buserite < Na-birnessite < Ba-buserite. Ba-buserite shows the highest specific area 93.64 m^2/g followed by Na-birnessite with 75.57 m^2/g and Sr-buserite 49.16 m^2/g. The complementary Ar-sorptiometric measurements for Na-birnessite and Ba-buserite recorded for a relative pressure of 0.05 exhibited slightly lower initial adsorption volumes compared to the N_2 adsorption data. Ba-buserite showed the highest adsorption volume of 17 cm^3/g, compared to 14 cm^3/g for Na-birnessite. A mean diameter of 7 Å obtained by the differential pore distribution calculated according to the Horvath-Kawazoe equation reinforced the conclusion regarding the instability of the Sr- and Ba-buserites at ambient

conditions and emphasized their partial or total conversion into the respective birnessites. Complementary BET specific area determination based on Ar-sorptiometric measurements showed a higher specific area in the case of Ba-birnessite compared to Na-birnessite. The latter, show a higher specific aree compared to the external surface, meanwhile the opposite was observed for Ba-buserite. The BET surface area determined for Ba-buserites was inferior in comparison to the one indicated in the literature concluding that the claimed as Ba-buserite was probably an intermediate of Na-birnessite and Ba-buserite. The adsorptive/exchanging properties of birnessites and buserites toward alkali- and transition heavy metal cations, for the remedy of the environment from their contamination are emphasized.

4. Conclusions

We reported in this study the synthesis of Na--birnessite and the attempt of the synthesis of Sr- and Ba-buserites. The synthesized samples revealed significant differences in their XRD powder patterns. The XRD pattern of the Na--birnessites matched well with the literature reported pattern, assigning it hence to the monoclinic system. The claimed Sr- and Ba-buserite patterns displayed also close similarities with reported ones. The N_2 adsorption measurements unveiled the presence of micropores in all samples. The overall external porosity of them increased in the order Sr-buserite < Na-birnessite < Ba-buserite. Ba-buserite shows the highest specific area 93.64 m^2/g followed by Na-birnessite with 75.57 m^2/g and Sr-buserite 49.16 m^2/g. The complementary Ar-sorptiometric measurements for Na-birnessite and Ba-buserite recorded for a relative pressure of 0.05 exhibited slightly lower initial adsorption volumes compared to the N_2 adsorption data. Ba-buserite showed the highest adsorption volume of 17 cm^3/g, compared to 14 cm^3/g for Na-birnessite. A mean diameter of 7 Å obtained by the differential pore distribution calculated according to the Horvath-Kawazoe equation reinforced the conclusion regarding the instability of the Sr- and Ba-buserites at ambient conditions and emphasized their partial or total conversion into the respective birnessites. Complementary BET specific area determination based on Ar-sorptiometric measurements showed a higher specific area in the case of Ba-birnessite compared to Na-birnessite. The latter show a higher specific surface compared to the external one, meanwhile the opposite was observed for Ba-buserite. The BET surface area determined for Ba-buserites was inferior in comparison to the one indicated in the literature concluding that the claimed as Ba-buserite was probably an intermediate of Na-birnessite and Ba-buserite. The adsorptive/exchanging properties of birnessites and buserites toward alkali- and transition heavy metal cations, for the remedy of the environment from their contamination are emphasized.

Acknowledgments

The financial support from Metallomic Scientific Network V4MSNet (project 11440027) is greatly acknowledged.

Conflicts of Interest

The authors declare they have no potential conflicts of interests concerning drugs, products,services or another research outputs in this study. The Editorial Board declares that the manuscript met the ICMJE „uniform reguirements“ for biomedical papers.

References

1. Jones, L. H. P., Milne, A. A. Mineral. Birnessite, a new manganese oxide mineral from Aberdeenshire, Scotland. Mineral. Mag., 1956, 31, 283-288.
2. Bricker, O. Some stability relations in system Mn-O2-H2O at 25 ºC and 1 atmosphere total pressure. Am. Mineral., 1965, 50, 1296-1354.
3. Giovanoli, R.; Burki, P. Comparison of X-ray evidence of marine manganese nodules and non-marine manganese ore deposits. Chimia, 1975, 29, 266-269.
4. Le Goff, P., Baffler, N., Bach, S., Pereira-Ramos, J. P. Synthesis, ion exchange and electrochemical properties of lamellar phyllomanganates of the birnessite group. Mat. Res. Bul., 1996, 31(1), 63-75.
5. Al-Attar, L., Dyer, A. Sorption behaviour of uranium on birnessite, a layered manganese oxide. J. Mater. Chem., 2002, 12, 1381-1386.
6. Golden, D. C., Chen C. C., Dixon, J. B. Transformation of birnessite to buserite, todorokite, and manganite under mild

hydrothermal treatment. Clays Clay Miner., 1987, 35(4), 271-280.
7. Luo, J., Zhang, Q., Huang, A., Giraldo, O., Suib, S. L. Double-Aging Method for Preparation of Stabilized Na-Buserite and Transformations to Todorokites Incorporated with Various Metals. Inorg. Chem., 1999, 38, 6106-6113.
8. Jeffries, D. S., Stumm, W. The metal-adsorption chemistry of buserite. Can.Mineral., 1976, 14, 16-22.
9. Mc Kenzie, R.M. The adsorption of lead and other heavy metals on oxides of manganese and iron. Aust. J. Soil Res., 1980, 18, 61-73.
10. Rives, V., Del Arco, M., Prieto, O. Birnesitas obtenidas mediante cambio iónico. Evolución estructural con la calcinación. (Birnessites obtained through ionic exchange. Structural evolution with the calcination). Bol. Soc. Esp. Ceram. V., 2004, 43(2), 142-147.
11. Feng, X. H., Zhai, L. M., Tan, W. F., Liu, F., He, J. Z. Adsorption and redox reactions of heavy metals on synthesized Mn oxide minerals. Environ Pollut., 2007, 147(2), 366-73.
12. Dias, A., Sá, R. G., Spitale, M. C., Athayde, M., Ciminelli, V. S.T. Microwave-hydrothermal synthesis of nanostructured Na-birnessites and phase transformation by arsenic(III) oxidation. Mat. Res. Bul., 2008, 43, 1528-1538.
13. Zhao, W., Wang, Q.Q., Liu, F. Pb2+ adsorption on birnessite affected by Zn2+ and Mn2+ pretreatments. J. Soils Sediment., 2010, 10, 870-878.
14. Pereira-Ramos, J. P., Badour, R., Bach, S., Baffier, N. Electrochemical and structural characteristics of some lithium intercalation materials synthesized via a sol-gel process: V2O5 and manganese dioxides-based compounds. Solid State Ionics, 1992, 701, 3-56.
15. Bach, S., Pereira-Ramos, J. P., Baffier, N. Electrochemical sodium insertion into the sol-gel birnessite manganese dioxide. Electrochim. Acta, 1993, 38, 1695-1700.
16. Bach, S., Pereira-Ramos, J. P., Baffier, N. Synthesis and Characterization of Lamellar MnO2 Obtained from Thermal Decomposition of NaMnO4 for Rechargeable Lithium Cells. J. Solid State Chem., 1995, 120, 70-73.
17. Shen, Y. F., Zerger, R. P., DeGuzman, R. N., Suib, S. L., McCurdy, L., Potter, D. I.; O'Young, C. L. Manganese oxide octahedral molecular sieves: preparation, characterization, and applications. J. Chem. Soc., Chem. Commun., 1992, 1213-1214.
18. Jiang, S. P., Ashton, W. R., Tseung, A. C. C. An observation of homogeneous and heterogeneous catalysis processes in the decomposition of H2O2 over MnO2 and Mn(OH)2. J. Catal., 1991, 131, 88-94.
19. Nitta, M. Characteristics of manganese nodules as adsorbents and catalysts, a review. Appl. Catal., 1984, 19, 151-176.
20. Yin, Y. G., Xu, W. Q., Shen, Y. F., Suib, L. S. Studies of Oxygen Species in Synthetic Todorokite-like Manganese Oxide Octahedral Molecular Sieves. Chem. Mater., 1994, 6(10), 1803-1808.
21. Wong, S.-T., Cheng, S. Synthesis and Characterization of Pillared Buserite. Inorg. Chem., 1992, 31, 1165-1172.
22. Gaillot, A.C., Drits, V.A., Manceau, A., Lanson, B. Structure of the synthetic K-rich phyllomanganate birnessite obtained by high-temperature decomposition of KMnO4: substructures of K-rich birnessite from 1000 ºC experiment. Micropor. Mesopor. Mat., 2007, 98, 267-282.
23. Tebo, B.M., Bargar, J.R., Clement, B.G., Dick, G.J., Murray, K.J., Parker, D., Verity, R., Webb, S.M. Biogenic manganese oxides: properties and mechanisms of formation. Annu. Rev. Earth Planet. Sci., 2004, 32, 287-328.
24. Murray, D. J., Healey T. W., Fuerstenau, D. W. The adsorption of aqueous metal on colloidal hydrous manganese oxide. In Advances in Chemistry, Series 79, Adsorption from Aqueous Solution. Amer. Chem. Soc., 1968, 74-81.
25. Post, J. E., Veblen, D. R. Crystal-structure determinations of synthetic sodium, magnesium, and potassium birnessite using TEM and the Rietveld method. Am. Miner., 1990, 75, 477.
26. Prieto, O., Rives, V. Preparation and characterization of nonstoichiometric manganese oxides. Bol. Soc. Esp. Cerám. Vidrio, 2000, 39(3), 233-238.
27. Brock, S. L., Duan, N., Tian, Z. R., Giraldo, O., Zhou H., Suib. S. L. A review of porous manganese oxide materials. Chem. Mater., 1998, 10, 2619-2628.
28. K. Kuma, A. Usui, W. Palawsky, B. Gedulin y G. Arrhenius. "Crystal structure of synthetic 7 Å and 10 Å manganates substituted by mono- and divalent cations". Miner. Mag., 1994, 58, 425-447.
29. Breck, D. W. Zeolite Molecular Sieves; Wiley: New York, 1973, pp 636.
30. Cornell, R. M., Giovanoli, R. Transformation of hausmannite into birnessite in alkaline media. Clays Clay Miner., 1988, 36(3), 249-257.
31. Shannon, R. D. Revised Effective Ionic Radii and Systematic Studies of Interatomic Distances in Halides and Chalcogenides. Acta Cryst., 1976, A32, 751-767.
32. Villalobos, M., Bargar, J., Sposito, G., Mechanisms of Pb(II) sorption on a biogenic manganese oxide. Environ. Sci. & Technol., 2005, 39, 569-576.